

# An integer-valued time series model for multivariate surveillance

Xanthi Pedeli

Department of Environmental Sciences, Informatics & Statistics  
Ca' Foscari University of Venice,  
Italy

Dimitris Karlis

Department of Statistics,  
Athens University of Economics  
Greece

## Abstract

In recent days different types of surveillance data are becoming available for public health reasons. In most cases several variables are monitored and events of different types are reported. As the amount of surveillance data increases, statistical methods that can effectively address multivariate surveillance scenarios are demanded. Even though research activity in this field is increasing rapidly in recent years, only a few approaches have simultaneously addressed the integer-valued property of the data and its correlation (both time correlation and cross correlation) structure. In this paper, we suggest a multivariate integer-valued autoregressive model that allows for both serial and cross correlation between the series and can easily accommodate overdispersion and covariate information. Moreover, its structure implies a natural decomposition into an endemic and an epidemic component, a common distinction in dynamic models for infectious disease counts. Detection of disease outbreaks is achieved through the comparison of surveillance data with one-step-ahead predictions obtained after fitting the suggested model to a set of clean historical data. The performance of the suggested model is illustrated on a trivariate series of syndromic surveillance data collected during Athens 2004 Olympic Games.

*Keywords:* count data; correlation; integer-valued time series; multivariate surveillance

## 1 Introduction

The main purpose of public health surveillance systems is the effective and timely detection of a disease outbreak so that control measures for the elimination of disease transmission can be rapidly taken. Over the last two decades, several statistical techniques such as statistical process control methods and statistical modelling techniques have been developed

to this direction Sonesson and Bock (2003); Shmueli and Burkom (2010); Unkel et al. (2012). These methods aim to identify unusual patterns in data series which may result from infectious disease outbreaks. Particular features that characterize these data series actually pose the statistical challenges in this research area.

More specifically, health data typically consist of non-negative counts representing numbers of events at specific time points. Consider for example the daily number of diagnosed cases or emergency department visits. In such cases, the normality assumption, that is fundamental for the construction of traditional control charts, is rather inappropriate and should be replaced by other, more suitable assumptions, like those of Poisson or negative binomial distributed data. The Poisson CUSUM Lucas (1985) and Poisson EWMA Borror et al. (1998) charts consist early adaptations of control charts for count data. Regression models with non-normal errors have also been suggested in the syndromic surveillance literature. Examples include Poisson log-linear models Parker (1989); Farrington et al. (1996); Jackson et al. (2007) and the count data regression charts constructed under the assumption of a generalized linear model for negative binomial counts Höhle and Paul (2008).

Another issue concerning data used in public health surveillance is that health data are usually correlated over time. Failure to account properly for autocorrelation can result in a misspecified model, introducing bias in the estimated effects and prediction intervals. In order to capture the correlation structure of health data, time series techniques have been used in the field of public health surveillance and outbreak detection. More often, autoregressive integrated moving average (ARIMA) models have been employed to model the variation of health data and their dependence on past observations Choi (1999); Helfenstein (1986); Watier et al. (1991); Reis and Mandl (2003). More sophisticated approaches as for example Bayesian and Hidden Markov models have also been suggested Strat and Carrat (1999); Held et al. (2006); Höhle (2007); Höhle and Mazick (2010). Extensive accounts of time series models and their limitations in public health surveillance (e.g. non-stationarity of surveillance data) can be found in Unkel et al. (2012) and Siripanthana (2013).

Generally, monitoring of a single series is of limited interest for outbreak detection purposes. For the early detection of a large-scale bioterrorism or epidemic outbreak, multivariate data should be considered. Such data can be a specific variable measured in several regions, or different variables measured in a particular region, or multiple variables measured in multiple regions (Siripanthana, 2013). In all these situations, the same underlying process may have generated several data series introducing correlations between them. To account for such correlations, and hence improve the timeliness in outbreak detection, multivariate surveillance has been proposed. Statistical methods used in multivariate surveillance are categorized into the following groups Sonesson and Friséen (2005); Friséen (2010): dimensionality reduction (including principal components and sufficient reduction techniques), parallel surveillance (where each series is monitored separately by means of a univariate surveillance method), joint modeling (with alarm functions based on the likelihood ratio statistic), scalar accumulation (Hotelling's  $T^2$  charts) and vector accumulation methods (MCUSUM and MEWMA charts). For multivariate counts Held et al. (2017) use

an observation driven model for surveillance, see also the work of Salmon et al. (2016) for related material. The approach of Schiöler and Friséen (2012) for continuous outcomes is also relevant.

Even though research activity in the field of multivariate surveillance increases rapidly in recent years, only a few approaches have simultaneously addressed the integer-valued property of the data and its correlation structure. Closest to such a comprehensive approach are the works of Held et al. (2005); Paul et al. (2008) and Paul and Held (2011) who use multivariate branching processes for modeling multivariate infectious disease surveillance data. In this paper, we suggest a different modeling approach based on the class of integer-valued autoregressive (INAR) processes. INAR models have been used in the context of health surveillance and outbreak detection by a few authors in the past. In a paper by Cardinal et al. (1999) INAR and ARIMA models are both applied for the analysis of infectious disease incidence and it is shown that the relative forecast error is smaller in the first instance. In a statistical process control framework, Weiß (2009, 2011) and Weiß and Testik (2009) proposed EWMA and CUSUM charts respectively for Poisson INAR(1) processes. For monitoring multivariate Poisson counts one can see the works of Cozzucoli and Marozzi (2018) and Wang et al. (2017).

In the context of multivariate health surveillance, a sufficient reduction method has been suggested Siripanathana (2013) for the detection of a shift in a bivariate Poisson INAR(1) process (Pedeli and Karlis, 2011). We take another perspective where a multivariate INAR(1) model is fitted to health data in order to make a prediction as a threshold for the next count. We consider a simplified version of the multivariate INAR(1) process proposed by Pedeli and Karlis (2013b) where the innovations  $\epsilon_t$  are assumed to be independent random variables. The introduced process has several merits. Firstly, it admits a realistic epidemiological interpretation especially for spatial and syndromic surveillance. Secondly, it accounts for the relationship with time lag between series, which is typical in disease transmission. Finally, it can easily accommodate overdispersion and covariate information and is extremely advantageous in terms of practical implementation.

The rest of the paper is organized as follows. Section 2 summarizes main concepts on multivariate integer-valued autoregressive processes and outlines the model and its properties. The suggested methodology is described in Section 3. Section 4 includes a simulation study for the evaluation of the suggested outbreak detection statistical process. A multivariate series of syndromic surveillance data illustrates our approach in Section 5. Section 6 concludes the paper.

## 2 Multivariate integer-valued autoregressive models

Integer-valued autoregressive (INAR) models have been introduced in the statistical literature by McKenzie (1985) and Al-Osh and Alzaid (1987) as discrete counterparts of the standard Gaussian autoregressive process. The simplest integer-valued autoregressive model is that of order one, denoted briefly as INAR(1) and defined as  $X_t = \alpha \circ X_{t-1} + \epsilon_t$ ,  $t \in \mathbb{N}$ ,

where  $\{\epsilon_t\}$  is an innovation process consisting of uncorrelated non-negative integer-valued random variables with finite mean and variance. The  $\circ$  symbol denotes the binomial thinning operator defined by  $\alpha \circ X = \sum_{j=1}^X Y_j$  where  $\{Y_j\}$  are independent identically distributed Bernoulli random variables with  $P(Y_j = 1) = 1 - P(Y_j = 0) = \alpha$ . The binomial thinning operator preserves the integer nature of the INAR process and introduce serial dependence though conditioning on  $X_{t-1}$ . In recent years, the wide interest in the class of INAR models has resulted in its enrichment with several variants and extensions of the benchmark integer-valued autoregressive model of order one. We concentrate on multivariate extensions of the INAR(1) process as considered by Pedeli and Karlis (2013b) and Pedeli and Karlis (2013a) and briefly summarized in the following.

**Full multivariate INAR(1) model** Assume that  $\mathbf{A}$  is a  $n \times n$  matrix with entries  $\alpha_{ij}$  satisfying  $0 \leq \alpha_{ij} \leq 1$  for  $i, j = 1, \dots, n$  and let  $\mathbf{X}$  be a random vector with values in  $\mathbb{N}^n$ . Then,  $\mathbf{A} \circ \mathbf{X}$  is a  $n$ -dimensional random vector with  $i$ -th component

$$[\mathbf{A} \circ \mathbf{X}]_i = \sum_{j=1}^n \alpha_{ij} \circ X_j, \quad i = 1, \dots, n \quad (1)$$

where the counting series in all  $\alpha_{ij} \circ X_j$ ,  $i, j = 1, \dots, n$  are assumed to be independent. Based on (1) we can define a full multivariate integer-valued autoregressive process of order 1 (MINAR(1)) (Pedeli and Karlis, 2013b)

$$\mathbf{X}_t = \mathbf{A} \circ \mathbf{X}_{t-1} + \epsilon_t, \quad t \in \mathbb{Z}, \quad (2)$$

where  $\{\epsilon_t\}_{t \in \mathbb{Z}}$  is a sequence of non-negative integer-valued random vectors, with mean  $\boldsymbol{\mu}_\epsilon$  and variance matrix  $\boldsymbol{\Sigma}_\epsilon$ , independent of  $\mathbf{A} \circ \mathbf{X}_{t-1}$ . Therefore, the  $i$ th element of the full MINAR(1) process is given by  $X_{it} = \sum_{j=1}^n \alpha_{ij} \circ X_{j,t-1} + \epsilon_{it}$ ,  $i = 1, \dots, n$ , where  $\alpha_{ij} \circ X$  are assumed to be mutually independent binomial thinning operations. The non-negative integer-valued random process  $\{\mathbf{X}_t\}_{t \in \mathbb{Z}}$  is the unique strictly stationary solution of (2) if the largest eigenvalue of  $\mathbf{A}$  is less than 1 and  $E\|\epsilon_t\| < \infty$ .

Using basic thinning operation properties (Franke and Rao, 1993; Latour, 1997), it can be shown that the mean vector and variance covariance matrix of the process  $\mathbf{X}_t$  are given by

$$\boldsymbol{\mu} = E(\mathbf{X}_t) = (\mathbf{I} - \mathbf{A})^{-1} \boldsymbol{\mu}_\epsilon, \quad (3)$$

and

$$\begin{aligned} \gamma(h) &= E[(\mathbf{X}_{t+h} - \boldsymbol{\mu})(\mathbf{X}_t - \boldsymbol{\mu})^T] \\ &= \begin{cases} \mathbf{A}\gamma(0)\mathbf{A}^T + \text{diag}(\mathbf{B}\boldsymbol{\mu}) + \boldsymbol{\Sigma}_\epsilon, & h = 0 \\ \mathbf{A}^h\gamma(0), & h \geq 1 \end{cases} \end{aligned} \quad (4)$$

respectively, where  $[\mathbf{B}]_{ij} = \alpha_{ij}(1 - \alpha_{ij})$  for  $i, j = 1, \dots, n$  (Pedeli and Karlis, 2013b).

The unknown parameter  $\boldsymbol{\theta} = (\text{vec}(\mathbf{A})', \boldsymbol{\mu}_\epsilon', \text{vec}(\boldsymbol{\Sigma}_\epsilon)')'$  of the full MINAR(1) process can be estimated using the method of conditional maximum likelihood (Pedeli and Karlis,

2013b). The maximum likelihood estimator (MLE) of  $\theta$  is defined as  $\hat{\theta} = \operatorname{argmax}_{\theta} \ell(\theta)$  where

$$\ell(\theta) = \sum_{t=2}^T \log f(\mathbf{x}_t | \mathbf{x}_{t-1}, \theta), \quad (5)$$

is the conditional log likelihood function and  $T$  is the length of the time series. The conditional densities involved in the right-hand side of (5) are convolutions of  $n$  sums of binomials  $f_i(x_i | \mathbf{x}_{t-1}) = P(X_{it} = x_i | \mathbf{X}_{t-1} = \mathbf{x}_{t-1})$ ,  $i = 1, \dots, n$ , and a distribution of the form  $g(k_1, \dots, k_n) = P(\epsilon_{1t} = k_1, \dots, \epsilon_{nt} = k_n)$ , corresponding to the joint distribution of the innovations  $\{\epsilon_t\}$ . Hence,  $f(\mathbf{x}_t | \mathbf{x}_{t-1}, \theta)$  can be expressed as the multiple sum

$$f(\mathbf{x}_t | \mathbf{x}_{t-1}, \theta) = \sum_{k_1=0}^{m_1} \cdots \sum_{k_n=0}^{m_n} f_1(x_{1t} - k_1 | \mathbf{x}_{t-1}) \cdots f_n(x_{nt} - k_n | \mathbf{x}_{t-1}) g(k_1, \dots, k_n),$$

where  $m_i = \min(x_{it}, x_{i,t-1})$ ,  $i = 1, \dots, n$ .

**Constrained multivariate INAR(1) model** For the maximization of (5) one can resort to numerical techniques. However, under the assumption of a cross-correlated innovation process, the complexity of (2) and hence the numerical difficulty of the maximum likelihood approach, increase sharply with dimensional increase (Pedeli and Karlis, 2013b). To avoid such complications, Pedeli and Karlis (2013a) consider a constrained MINAR(1) model by assuming a single source of dependence between the univariate series that comprise the MINAR(1) process. In particular,  $\mathbf{A}$  is assumed to be a  $n \times n$  diagonal matrix with independent elements  $\alpha_i = [\mathbf{A}]_{ii}$ ,  $i = 1, \dots, n$ , while  $\{\epsilon_t\}$  follow jointly a discrete multivariate distribution. One can easily see that the assumption of a diagonal  $\mathbf{A}$  matrix significantly reduces the correlation structure since each univariate series  $\{X_{it}\}$  at time  $t$  is a function of each own predecessors at time  $t - 1$  but not of the predecessors of the rest of the series comprising the MINAR(1) process, i.e.  $X_{it} = \alpha_i \circ X_{i,t-1} + \epsilon_{it}$ ,  $i = 2, \dots, n$ . For the estimation of this simplified model, Pedeli and Karlis (2013a) suggest a pairwise likelihood approach that reduces the multivariate estimation problem to a set of bivariate problems.

### 3 Surveillance using a new MINAR(1) specification

Traditionally, statistical models for health surveillance data aim to effectively capture the endemic and epidemic dynamics of disease risk. In principle, the endemic component explains a baseline rate of cases with stable temporal pattern. More specifically, it describes the risk of new events as a function of external factors independent of the history of the epidemic process. Seasonality, socio-demographic characteristics, population density and vaccination coverage are a few examples of such factors. The epidemic component on the other hand aims to introduce infectiousness, that is explicit dependence between events. Therefore the epidemic component is driven by the observed past and is identified with the autoregressive part of the model (Meyer et al., 2017).

This additive decomposition of disease risk is well embodied in model (2). However, the simplification of (2) based on the assumption of a diagonal matrix  $\mathbf{A}$  weakens the ability of the model to capture the epidemic dynamics of disease risk since it ignores the relationship with time lag between series that is typical in disease transmission. Moreover, inference for the constrained multivariate INAR(1) model is based on a pairwise likelihood approach Pedeli and Karlis (2013a) which is not appropriate for prediction purposes since the accuracy of the predictive conclusions is affected by the fact that they are based on a misspecified model (misspecification error).

To balance between effectiveness and attractiveness of the model, we consider here another simplification of (2). In particular, we assume that the correlation matrix  $\mathbf{A}$  is non-diagonal and we relax the degree of complexity of the model by assuming that the innovation series  $\epsilon_t$ , i.e. the endemic components, are uncorrelated. The resulting model admits a realistic epidemiological interpretation and is extremely advantageous in terms of practical implementation since the distribution of the innovations becomes a product of univariate mass functions, i.e.

$$g(k_1, \dots, k_n) = \prod_{i=1}^n P(\epsilon_{it} = k_i).$$

The mean vector and variance covariance matrix of the new MINAR(1) process  $\mathbf{X}_t$  are still given by (3) and (4) respectively where  $\Sigma_\epsilon$  is now a diagonal matrix.

Moreover, overdispersion that is a typical characteristic of health surveillance data, can be easily accommodated even under the simplest parametric assumption of Poisson innovations. More specifically, in line with Pedeli and Karlis (2013a) it can be proved that if  $\epsilon_t = (\epsilon_{1t}, \dots, \epsilon_{nt})'$  are independent Poisson random variables with parameters  $\lambda = (\lambda_1, \dots, \lambda_n)'$ , then the joint distribution of  $\mathbf{X}_t$  is given by the product of  $n$  generalized Poisson distributions Gurland (1957); Kemp and Kemp (1965) with parameters that are nonlinear combinations of  $\lambda$  and powers of  $\mathbf{A}$ . In the bivariate case ( $n = 2$ ), it is straightforward to show that the vector of expectations  $\mu = (\mu_1, \mu_2)'$  and the variance covariance matrix  $\gamma(0) = \begin{bmatrix} \gamma_{11}(0) & \gamma_{12}(0) \\ \gamma_{12}(0) & \gamma_{22}(0) \end{bmatrix}$  have elements

$$\mu_1 = \frac{(1 - \alpha_{22})\lambda_1 + \alpha_{12}\lambda_2}{(1 - \alpha_{11})(1 - \alpha_{22}) - \alpha_{12}\alpha_{21}}, \quad \mu_2 = \frac{(1 - \alpha_{11})\lambda_2 + \alpha_{21}\lambda_1}{(1 - \alpha_{11})(1 - \alpha_{22}) - \alpha_{12}\alpha_{21}},$$

and

$$\begin{aligned} \gamma_{11}(0) &= \frac{(1 - \alpha_{11}^2)\mu_1 + \alpha_{12}^2(\gamma_{22}(0) - \mu_2) + 2\alpha_{11}\alpha_{12}\gamma_{12}(0)}{1 - \alpha_{11}^2}, \\ \gamma_{22}(0) &= \frac{(1 - \alpha_{22}^2)\mu_2 + \alpha_{21}^2(\gamma_{11}(0) - \mu_1) + 2\alpha_{22}\alpha_{21}\gamma_{12}(0)}{1 - \alpha_{22}^2}, \\ \gamma_{12}(0) &= \frac{\alpha_{11}\alpha_{21}\gamma_{11}(0) + \alpha_{22}\alpha_{12}\gamma_{22}(0)}{1 - \alpha_{11}\alpha_{22} - \alpha_{12}\alpha_{21}}, \end{aligned}$$

respectively. For higher dimensions, we confine to the general formulae (3) and (4) since closed form expressions for the elements of  $\boldsymbol{\mu}$  and  $\boldsymbol{\gamma}(0)$  cannot be easily derived. Other parametric families, as e.g. the negative binomial distribution, can also be easily considered for the distribution of the innovations depending on the degree of overdispersion present in the data.

Conditional maximum likelihood estimates for the new MINAR(1) process can be obtained through maximization of the likelihood function

$$L(\boldsymbol{\theta}|\mathbf{x}) = \prod_{t=2}^T f(\mathbf{x}_t|\mathbf{x}_{t-1}, \boldsymbol{\theta}),$$

where  $f(\mathbf{x}_t|\mathbf{x}_{t-1}, \boldsymbol{\theta})$  is the conditional density of  $\mathbf{X}_t$  given  $\mathbf{X}_{t-1}$  and  $\boldsymbol{\theta}$  is the vector of unknown parameters. For instance, in the bivariate case and under the assumption of Poisson innovations,

$$\begin{aligned} f(\mathbf{x}_t|\mathbf{x}_{t-1}, \boldsymbol{\theta}) = & \sum_{k_1=0}^{\min(x_{1t}, x_{1,t-1}, x_{2,t-1})} \sum_{k_2=0}^{\min(x_{2t}, x_{1,t-1}, x_{2,t-1})} \left\{ e^{-(\lambda_1+\lambda_2)} \sum_{m=0}^{\min(k_1, k_2)} \frac{\lambda_1^{x_{1t}-k_1-m} \lambda_2^{x_{2t}-k_2-m}}{(x_{1t}-k_1-m)!(x_{2t}-k_2-m)!} \right. \\ & \times \sum_{j_1=0}^{k_1} \binom{x_{1,t-1}}{j_1} \binom{x_{2,t-1}}{k_1-j_1} \alpha_{11}^{j_1} (1-\alpha_{11})^{x_{1,t-1}-j_1} \alpha_{12}^{k_1-j_1} (1-\alpha_{12})^{x_{2,t-1}-k_1+j_1} \\ & \left. \times \sum_{j_2=0}^{k_2} \binom{x_{2,t-1}}{j_2} \binom{x_{1,t-1}}{k_2-j_2} \alpha_{22}^{j_2} (1-\alpha_{22})^{x_{2,t-1}-j_2} \alpha_{21}^{k_2-j_2} (1-\alpha_{21})^{x_{1,t-1}-k_2+j_2} \right\} \end{aligned}$$

where  $\boldsymbol{\theta} = \{\alpha_{11}, \alpha_{12}, \alpha_{21}, \alpha_{22}, \lambda_1, \lambda_2\}$ . If other parametric assumptions are made as e.g. negative binomial innovations, the above formula can be modified accordingly.

The newly defined multivariate INAR(1) process can be used for modeling clean historical data and make one-step-ahead forecasts that can be used for prediction-based monitoring. We should emphasize here that the set-up phase is assumed to be free or cleaned of outbreaks. The suggested outbreak detection statistical process comprises of two steps: In the first step, the available series of data in the set-up phase (historical data) is modeled through a multivariate INAR(1) process and a parameter vector of maximum likelihood estimates  $\hat{\boldsymbol{\theta}}$  is obtained. The second step is dedicated to the successive monitoring of incoming observations in the operational phase (surveillance data) using the model obtained from the set-up phase. In particular, the actually observed realization  $\mathbf{x}_{t+1}$  is assessed against a multivariate prediction threshold derived from the model fitted in the first step in order to define whether an alarm should be triggered. More specifically, for each multivariate observation  $\mathbf{x}_{t+1}$  in the operational phase, we estimate the one-step-ahead predictive distribution  $\hat{P}(\mathbf{X}_{t+1} = \mathbf{x}_{t+1}|\mathbf{x}_t, \hat{\boldsymbol{\theta}})$ ,  $\mathbf{x} \in \mathbb{N}_0^n$  and obtain the marginal predictive probabilities  $\hat{P}(X_{i,t+1} = x_{i,t+1}|\mathbf{x}_t, \hat{\boldsymbol{\theta}})$ ,  $i = 1, \dots, n$ . For each observation  $X_{i,t+1}$ , we construct an  $(1-\alpha)\%$  prediction interval with upper bound  $x_{i,t+1}^{UB}$  equal to the  $(1-\alpha)$ -quantile of the corresponding marginal predictive distribution, where  $\alpha$  is a prespecified significance level. The lower bound of the prediction interval is set equal to 0 since we are only interested in detecting

positive deviations from the in-control model. Each series flags an alarm at time  $t + 1$  if the corresponding observation lies outside the prediction interval, i.e. if

$$x_{i,t+1} > x_{i,t+1}^{UB}.$$

Finally, for the overall alarm, a majority rule can be defined, i.e. flagging an alarm if a certain percentage of the series signals an alarm at the same point in time (Vial et al., 2016).

## 4 Simulation study

We conducted a small simulation study aiming to evaluate the performance of the suggested outbreak detection statistical process. Time series data of length  $n = 200$  were simulated from a trivariate INAR(1) model with independent Poisson innovations. We assumed that the first 150 observations consist the set-up phase (that is a clean process without outbreaks) and the last 50 observations consist the monitoring phase. Subsequently, for each series  $i$ ,  $i = 1, 2, 3$ , we simulated an outbreak of expected size  $\kappa_i$  at time  $t = 170$  from a Poisson distribution with mean equal to  $\kappa_i$ . Therefore, our model has the form

$$\begin{pmatrix} X_{1t} \\ X_{2t} \\ X_{3t} \end{pmatrix} = \begin{bmatrix} \alpha_{11} & \alpha_{12} & \alpha_{13} \\ \alpha_{21} & \alpha_{22} & \alpha_{23} \\ \alpha_{31} & \alpha_{32} & \alpha_{33} \end{bmatrix} \circ \begin{pmatrix} X_{1,t-1} \\ X_{2,t-1} \\ X_{3,t-1} \end{pmatrix} + \begin{pmatrix} \epsilon_{1t} \\ \epsilon_{2t} \\ \epsilon_{3t} \end{pmatrix},$$

where  $\epsilon_{it}$  are independent Poisson random variables with mean  $E(\epsilon_{it}) = \lambda_i + \kappa_i I(t = 170)$  and  $I(A)$  is an indicator function.

The true parameter values were assumed to be

$$\mathbf{A} = \begin{bmatrix} \alpha_{11} & \alpha_{12} & \alpha_{13} \\ \alpha_{21} & \alpha_{22} & \alpha_{23} \\ \alpha_{31} & \alpha_{32} & \alpha_{33} \end{bmatrix} = \begin{bmatrix} 0.3 & 0.1 & 0.2 \\ 0.2 & 0.4 & 0.2 \\ 0.3 & 0.2 & 0.2 \end{bmatrix},$$

and  $\lambda_1 = \lambda_2 = \lambda_3 = 1$ . We also assumed that  $\kappa_1 = \kappa_2 = \kappa_3 = \kappa$  and we took the values of  $\kappa$  to be 5, 8 or 10. By choosing these specific values for  $\kappa$  we aim to study both cases where the outbreak is manifest, as well as cases where the outbreak cannot be easily distinguished from the typical range of values in the in-control state. Figure 1 shows the cumulative distribution of the maximum values of 10000 trivariate INAR(1) series with independent Poisson innovations and  $n = 200$  observations. All trivariate series are free of outbreaks ( $\kappa = 0$ ) and have been simulated with parameter values as described above.

The maximum values range between 6 and 18 for  $\{X_1\}$  and  $\{X_2\}$  and between 7 and 21 for  $\{X_3\}$ . Since the process is in control until  $t = 169$ , the expected value of the trivariate series at the time of the outbreak ( $t = 170$ ) can be easily computed as  $E(\mathbf{X}_{170}) = \mathbf{A}E(\mathbf{X}_{169}) + \boldsymbol{\lambda} + \boldsymbol{\kappa} = \mathbf{A}(\mathbf{I} - \mathbf{A})^{-1}\boldsymbol{\lambda} + \boldsymbol{\lambda} + \boldsymbol{\kappa}$ , where  $\boldsymbol{\lambda} = (\lambda_1, \lambda_2, \lambda_3)'$ . The computed expectations for  $\kappa = 5, 8$  and 10 are summarized in Table 1 and illustrated in Figure 1 with vertical lines. Table 2 summarizes the empirical probabilities of the maximum value of each univariate series being greater than the corresponding expectation of



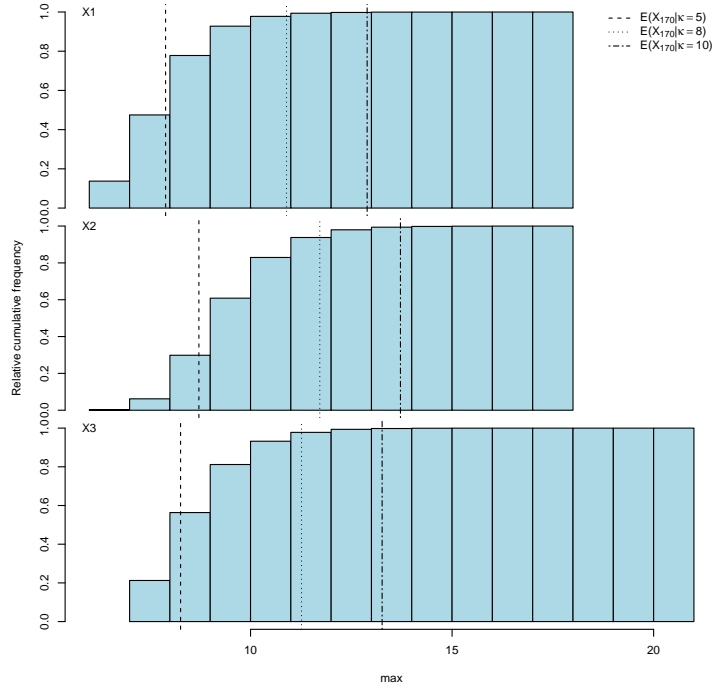


Figure 1: Cumulative distribution of the maximum values of 10000 triivariate INAR(1) series with independent Poisson innovations. Data have been simulated with  $n = 200$  and  $\alpha = (\alpha_{11}, \alpha_{12}, \alpha_{13}, \alpha_{21}, \alpha_{22}, \alpha_{23}, \alpha_{31}, \alpha_{32}, \alpha_{33}, \lambda_1, \lambda_2, \lambda_3) = (0.3, 0.1, 0.2, 0.2, 0.4, 0.2, 0.3, 0.2, 0.2, 1, 1, 1)$ .

the series at the time of an outbreak ( $t = 170$ ),  $P(\max_{i \neq 170} (x_{it}) > E(X_{i,170}))$ ,  $i = 1, 2, 3$ . From Figure 1 and Table 2 we can conclude that  $\kappa = 5$  corresponds to outbreaks that cannot be easily distinguished from the typical range of values in the in-control state, since the empirical probabilities  $P(\max_{i \neq 170} (x_{it}) > E(X_{i,170}))$  are high for all univariate series. In contrast,  $k = 8$  and  $k = 10$  correspond to pronounced outbreaks with small empirical probabilities.

For each scenario ( $\kappa = 5, 8$  or  $10$ ), we conducted 1000 simulation replicates. In each replicate, a trivariate INAR(1) model with independent Poisson innovations was fitted to the set-up phase and the parameter estimates were used to compute 90%, 95% and 99% upper prediction limits for the monitoring phase. For comparison purposes, we also fitted three independent INAR(1) models with Poisson innovations to the historical data and followed the same process for the computation of upper prediction limits.

As evaluation measures we used the detection rate and weekly false alarm rate based on a rule of 2/3 that is, assuming that an alarm is triggered if at least two out of the three series flagged an alarm at the same point in time. The detection rate was computed as the proportion of the 1000 replicates in which an alarm was triggered at time  $t = 170$  while the

Table 1: Expected values of a triivariate INAR(1) series with independent Poisson innovations at the time of an outbreak of expected size  $\kappa$  equal to 5,8 and 10. Assumed parameter values are equal to  $\vec{\alpha} = (\alpha_{11}, \alpha_{12}, \alpha_{13}, \alpha_{21}, \alpha_{22}, \alpha_{23}, \alpha_{31}, \alpha_{32}, \alpha_{33}, \lambda_1, \lambda_2, \lambda_3) = (0.3, 0.1, 0.2, 0.2, 0.4, 0.2, 0.3, 0.2, 0.2, 1, 1, 1)$ .

$\kappa$	$E(X_{1t})$	$E(X_{2t})$	$E(X_{3t})$
5	7.9	8.7	8.3
8	10.9	11.7	11.3
10	12.9	13.7	13.3

Table 2: Empirical probabilities of the maximum value of each univariate series being greater than the corresponding expectation of the series at the time of an outbreak of expected size  $\kappa$  equal to 5, 8 and 10. Data have been simulated with  $n = 200$  and  $\vec{\alpha} = (\alpha_{11}, \alpha_{12}, \alpha_{13}, \alpha_{21}, \alpha_{22}, \alpha_{23}, \alpha_{31}, \alpha_{32}, \alpha_{33}, \lambda_1, \lambda_2, \lambda_3) = (0.3, 0.1, 0.2, 0.2, 0.4, 0.2, 0.3, 0.2, 0.2, 1, 1, 1)$ . The outbreak is assumed to happen at time  $t = 170$ .

$\kappa$	$P(\max_{t \neq 170} x_{it} > E(X_{i,170}))$		
	$i = 1$	$i = 2$	$i = 3$
5	0.863	0.938	0.788
8	0.072	0.171	0.068
10	0.006	0.020	0.006

weekly false alarm rate was defined as the number of cases in which an alarm was flagged at time  $t \neq 170$  divided by  $1000 \times 49$ . Based on our simulations, we have also approximated the average run length (ARL) for different outbreak sizes  $\kappa$  and different significance levels  $\alpha$ . In particular, for each univariate series we used the standard definition of ARL that is, we defined  $ARL_i$ ,  $i = 1, 2, 3$  as the average number of points in the monitoring phase that precede the very first indication of a false alarm. Then, to get an overall measure of the performance of the suggested multivariate surveillance approach, we followed a conservative approach defining  $ARL = \min_i ARL_i$ . However, it is important to note that this approximation and the related results should be treated with caution, first of all due to the limited number of simulations Weiß (2015), secondly because we are handling multivariate count data through a multivariate surveillance approach, and thirdly because our decision on the occurrence of an outbreak is based on a 2/3 rule rather than on modelling each series separately.

The estimated  $ARL_i$ 's and ARLs are summarized in Table 3. The ARLs range from 12.6 to 13.1, 17.9 to 18.1 and 21.7 to 23.3 for  $\alpha = 10\%, 5\%$  and  $1\%$  respectively when the multivariate approach is applied. Keeping in mind that the true outbreak has actually occurred at  $t = 170$  and that the monitoring phase is the period  $t = 150, \dots, 200$ , we conclude that if a false alarm is triggered, this is expected to happen around a week earlier than the true outbreak when  $\alpha = 10\%$ , around the time of the true outbreak when  $\alpha = 5\%$  and a bit later than the time of the true outbreak when  $\alpha = 1\%$ . Fitting three independent INAR(1) models to the data results in generally lower ARLs that range between 10.1 and 10.3 when  $\alpha = 10\%$ , between 14.1 and 15.1 when  $\alpha = 5\%$  and between 19.5 and 21.6 when

Table 3: Average run lengths for the three series ( $ARL_i$ 's) and overall (ARLs), for different outbreak sizes  $\kappa$  and different significance levels  $\alpha$ .

Outbreak size	Sign. level	trivariate INAR(1)				independent INAR(1)			
		$ARL_1$	$ARL_2$	$ARL_3$	ARL	$ARL_1$	$ARL_2$	$ARL_3$	ARL
$\kappa = 5$	$\alpha = 10\%$	13.6	13.1	13.1	13.1	14.8	10.3	11.1	10.3
	$\alpha = 5\%$	18.4	18.7	17.9	17.9	19.0	15.1	16.0	15.1
	$\alpha = 1\%$	22.2	23.9	21.7	21.7	22.3	21.6	21.6	21.6
$\kappa = 8$	$\alpha = 10\%$	13.0	13.1	12.6	12.6	14.4	10.3	11.2	10.3
	$\alpha = 5\%$	18.5	18.5	18.1	18.1	18.4	15.0	15.8	15.0
	$\alpha = 1\%$	22.5	23.4	22.4	22.4	21.4	21.0	21.1	21.0
$\kappa = 10$	$\alpha = 10\%$	13.8	13.0	13.5	13.0	14.4	10.1	11.2	10.1
	$\alpha = 5\%$	18.1	18.7	18.8	18.1	18.8	14.1	15.3	14.1
	$\alpha = 1\%$	26.6	23.3	24.0	23.3	22.0	19.5	20.6	19.5

$\alpha = 1\%$ . The consistently higher ARLs obtained by the multivariate approach indicate its superiority over the univariate modeling approach in terms of this specific evaluation measure.

The estimated detection rates and false alarm rates are summarized in Table 4. As expected, the larger the size of the outbreak is, the higher the achieved detection rate. This conclusion holds for both the trivariate and the independent INAR(1) modeling approaches that are equivalently effective in terms of the estimated detection rates. However, the multivariate approach has an obvious superiority in terms of the false alarm rates that are consistently lower than the corresponding false alarms rates achieved for all  $\kappa$ 's and  $\alpha$ 's under the univariate approach. The outperformance of the multivariate approach in terms of false alarm rates is not surprising since the independent INAR(1) models ignore the cross-correlation between the series resulting in narrower prediction intervals and thus increasing the number of false alarms.

Focusing on the multivariate approach, it is evident that the false alarm rates are generally low without any particular pattern with regard to the outbreak size. Regarding the role of the significance level  $\alpha$ , we observe that decreasing  $\alpha$  results in lowering both the detection rates and false alarm rates. The degree of reduction depends however on the true outbreak size. In particular, the conservative  $\alpha = 1\%$  proves to be too strict for  $\kappa = 5$  as it achieves a detection rate of around 55% contrary to  $\alpha = 5\%$  or  $10\%$  that achieve detection rates of 80% and 89% respectively. However, the detection rates achieved at different significance levels improve considerably for larger outbreak sizes even reaching 99.8% for  $\kappa = 10$  and  $\alpha \geq 5\%$ . For  $\alpha = 1\%$  the corresponding detection rate is equal to 98.5% but with a false alarm rate of 0.03% that is much smaller than those corresponding to  $\alpha = 5\%$  or  $10\%$  (0.40% and 1.44% respectively). Conclusively, for the choice of the significance level to be used for outbreak detection purposes, one should consider the outbreak size that he or she would like to detect and the false alarm rate that is ready to accept. In the following section we use the conservative  $\alpha = 1\%$ .

Table 4: Detection rates (DR) and false alarm rates (FAR) for different outbreak sizes  $\kappa$  and different significance levels  $\alpha$ . The reported numbers have been multiplied by 100.

Outbreak size	Sign. level	trivariate INAR(1)		independent INAR(1)	
		DR	FAR	DR	FAR
$\kappa = 5$	$\alpha = 10\%$	89.0	1.33	88.6	2.95
	$\alpha = 5\%$	80.1	0.34	78.4	0.99
	$\alpha = 1\%$	55.1	0.01	49.5	0.10
$\kappa = 8$	$\alpha = 10\%$	99.4	1.30	99.3	3.80
	$\alpha = 5\%$	98.7	0.32	98.0	1.51
	$\alpha = 1\%$	93.4	0.01	91.4	0.23
$\kappa = 10$	$\alpha = 10\%$	99.8	1.44	99.9	4.22
	$\alpha = 5\%$	99.8	0.40	99.7	1.93
	$\alpha = 1\%$	98.5	0.03	98.1	0.36

## 5 Application using Syndromic data

Among various aspects of health surveillance, syndromic surveillance is considered as an important tool since it is based on symptoms rather than diagnosis and hence it can create alerts faster. For example, syndromic surveillance systems for detection of biologic terrorism after the terrorist attack of September 11, 2001 have been launched in New York city (Das et al., 2003). In addition, during large athletic events such surveillance systems can be useful to quickly detect threats for the public health, and they have been used in winter Olympic Games in Salt Lake City 2002 (Gesteland et al., 2003; Mundorff et al., 2004) and Athens 2004 Olympic Games (Dafni et al., 2004). Syndromic surveillance data are by nature low count data, especially if they refer to incidences of diseases and symptoms that are not so common. In such cases, the usual normal approximation is not appropriate and the data should rather be treated as discrete-valued time series. Moreover, when the collected data involve several related variables, this brings forward the need to consider multivariate surveillance techniques.

The data considered here is part of the syndromic surveillance data collected during Athens 2004 Olympic Games. The full database consists of eleven different syndromes recorded since July 2002 in emergency departments of major hospitals in the Greater Athens area (drop-in syndromic surveillance) (Dafni et al., 2004). For the purpose of the current analysis we consider three distinct syndromes recorded in a specific hospital that are significantly correlated to each other (cross-correlations ranging from 0.31 to 0.48). In particular, we consider respiratory infection with fever, febrile illness with rash and other syndrome with potential interest for public health. The latter is a general category including all symptoms that could not be classified in any of the other prespecified categories.

Our monitoring period starts on March 2, 2004 and ends on September 28, 2004 while the period between August 1, 2002 and August 29, 2003 is considered as the set-up phase. During both periods syndromes were recorded every three days so that the historical and surveillance data consist of  $t_0 = 127$  and  $t_1 = 71$  observations respectively. The time series plots of the three series during the set-up and monitoring phases are included in Figure 2. Table 5 summarizes basic descriptive statistics. The plots of autocorrelations and partial

autocorrelations of the three series during the set-up phase are shown in Figure 3. The exponentially decaying autocorrelation functions indicate the appropriateness of an AR-type modeling approach whilst the partial autocorrelation functions suggest an order of dependence around one or two.

In the following we apply the approach of Section 3, i.e. we fit a trivariate INAR(1) model with independent Poisson innovations for modeling and prediction using the historical syndromic surveillance data. To account for regressors usually related to infectious disease data we express the expectation of the innovation series as function of the available covariate information, i.e.  $E(\epsilon_{it}) = \exp(\mathbf{z}'_t \boldsymbol{\beta})$ ,  $i = 1, 2, 3$ , where  $\mathbf{z}_t$  as a vector of covariates with associated regression parameters  $\boldsymbol{\beta}$  (Pedeli and Karlis, 2013a). As candidate covariates we consider terms for seasonality and a binary indicator for the day of the week on which the recording of syndromes was implemented (weekdays vs. weekends). We don't consider time trends since Figure 2 does not suggest the presence of any trend in our data. Therefore, each marginal series is modeled as  $X_{it} = \sum_{j=1}^3 \alpha_{ij} \circ X_{j,t-1} + \epsilon_{it}$ ,  $i = 1, 2, 3$ , where  $\epsilon_{it}$  are independent Poisson random variables with mean

$$E(\epsilon_{it}) = \exp \left\{ \beta_{i0} + \beta_{i1} \text{Weekday} + \beta_{i2} \cos \left( \frac{2\pi t}{122} \right) + \beta_{i3} \sin \left( \frac{2\pi t}{122} \right) \right\} \quad (6)$$

for  $t = 1, \dots, t_0$ . Note that in the trigonometric terms that have been employed to capture seasonal patterns, we consider a seasonal period equal to 122 because our data are recorded in three-days intervals. For comparison purposes we also employ a univariate surveillance approach based on fitting three independent INAR(1) regression models with Poisson innovations. Covariate information is incorporated in the univariate models in the same way, i.e. through (6). With both approaches, the marginal one-step-ahead predictive distributions are used for the construction of  $(1 - \alpha)\%$  prediction intervals, the upper bounds of which serve as thresholds for outbreak detection. We assume a component-wise type I error rate of  $\alpha = 0.01$  and for the overall alarm we set a rule of 2/3 that is an alarm is triggered if at least two out of the three series flag an alarm at the same point in time.

The parameter estimates and corresponding standard errors obtained with the two modeling approaches are summarized in Table 6. Results indicate significant first-order autocorrelations under both fittings. The cross-correlation parameters estimated by the trivariate INAR(1) model are also significant indicating the appropriateness of the multivariate approach. Figure 4 shows the correlograms of the residuals obtained by the two modeling approaches. Obviously, the trivariate INAR(1) regression model can effectively capture significant autocorrelations at almost all lags while the three univariate INAR(1) models are less effective in accounting for autocorrelations greater than one. However, Figure 5 reveals some remaining cross-correlations with both approaches although such cross-correlations are more persistent with the univariate INAR(1) models.

The surveillance plots obtained under the two models are shown in Figure 6. Red dashed lines represent the upper bounds of the corresponding 99% prediction intervals while blue crosses indicate the time points at which an overall alarm is raised. The two alarms signalled with the trivariate INAR(1) fitting are also triggered when three indepen-

Table 5: Mean, variance and coefficient of variation (CV) for the three syndromes during the set-up and monitoring phases.

	Set-up phase			Monitoring phase		
	Mean	Variance	CV	Mean	Variance	CV
Respiratory infection	6.17	22.40	76.7%	9.90	18.46	43.4%
Febrile illness	5.76	19.96	77.5%	11.48	15.37	34.2%
Other syndrome	4.39	12.34	79.9%	4.89	10.36	65.9%

dent INAR(1) models are fitted to the historical data but the later approach also gives an additional alarm.

## 6 Discussion

As the amount of available data increases, multivariate surveillance scenarios become more and more plausible. Aiming to contribute in this developing area, we suggest a multivariate INAR(1) approach, suitable for joint modeling of multivariate surveillance data. The introduced model admits a realistic epidemiological interpretation with a clear distinction between the epidemic and endemic components and accounts for overdispersion that is typical with surveillance data. Even though emphasis has been put on the case of independent Poisson innovations, other discrete distributions, as e.g. the negative binomial, can also be considered instead.

In this paper we provided a generic framework for using models suitable for multivariate counts time series for surveillance purposes. A series of interesting points that refer to the context of surveillance can be further exploited, as for example updating the data basis for the model fit in a regular basis and keep the newest observations only for building the model (see Noufaily et al. (2013)) or downweight past outbreaks by suitable adjustments (e.g. in Noufaily et al. (2013) Anscombe residuals were used). Of course note that, because of the discreteness of the data, it is not obvious how methods suitable for continuous and univariate outcomes translate to our case and this is an interesting topic for further research.

A final comment relates to the parametric assumptions made in this paper. While our model can capture small to moderate overdispersion one may alter the assumption about the innovations to allow for larger overdispersion. Also note the notion of multivariate overdispersion discussed in Kokonendji and Puig (2018) which can be also a vehicle for building more flexible models and examine their properties.

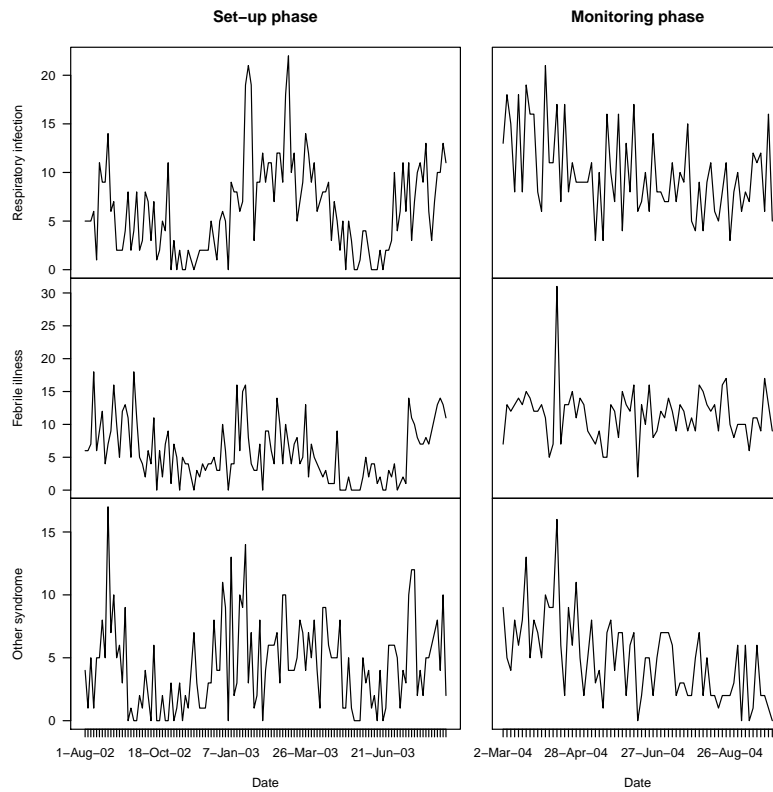


Figure 2: Time series plots of the data

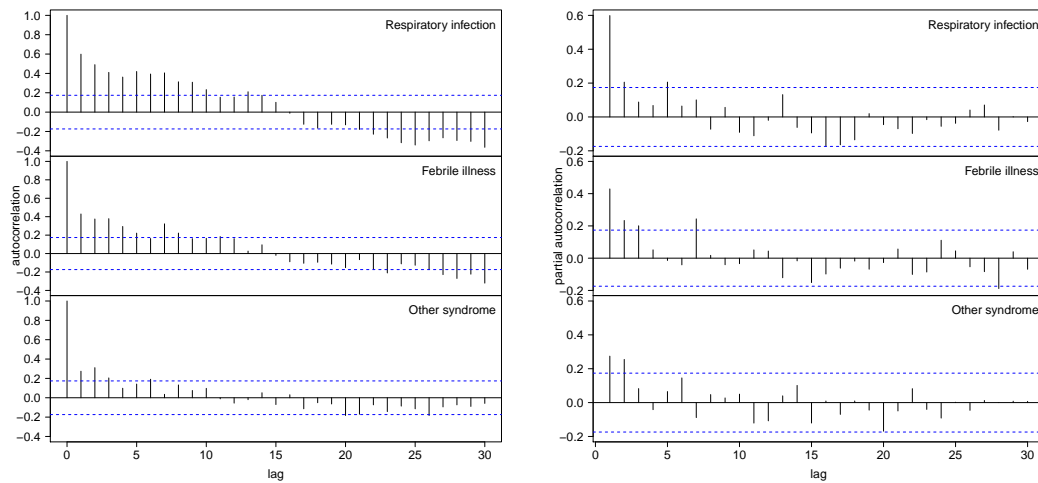


Figure 3: Plots of the autocorrelations (left panel) and partial autocorrelations (right panel) of the historical data

Table 6: Maximum likelihood estimates (standard errors) from fitting three independent Poisson INAR(1) or a trivariate INAR(1) regression model with independent Poisson innovations to the historical data.

correlation parameters	trivariate INAR(1)	independent INAR(1)	regression parameters	trivariate INAR(1)	independent INAR(1)
$\hat{\alpha}_{11}$	0.329 (0.044)	0.393 (0.039)	$\hat{\beta}_{10}$	1.190 (0.153)	1.506 (0.099)
$\hat{\alpha}_{12}$	0.126 (0.043)	-	$\hat{\beta}_{11}$	-0.255 (0.145)	-0.278 (0.110)
$\hat{\alpha}_{13}$	0.134 (0.054)	-	$\hat{\beta}_{12}$	-0.359 (0.118)	-0.222 (0.078)
$\hat{\alpha}_{21}$	0.160 (0.040)	-	$\hat{\beta}_{13}$	-0.218 (0.098)	-0.140 (0.073)
$\hat{\alpha}_{22}$	0.177 (0.045)	0.263 (0.041)	$\hat{\beta}_{20}$	1.197 (0.135)	1.496 (0.096)
$\hat{\alpha}_{23}$	0.141 (0.048)	-	$\hat{\beta}_{21}$	-0.267 (0.133)	-0.118 (0.102)
$\hat{\alpha}_{31}$	0.062 (0.039)	-	$\hat{\beta}_{22}$	0.411 (0.121)	0.156 (0.070)
$\hat{\alpha}_{32}$	0.108 (0.039)	-	$\hat{\beta}_{23}$	0.548 (0.110)	0.296 (0.068)
$\hat{\alpha}_{33}$	0.131 (0.047)	0.179 (0.045)	$\hat{\beta}_{30}$	0.990 (0.155)	1.246 (0.109)
			$\hat{\beta}_{31}$	0.047 (0.142)	0.046 (0.113)
			$\hat{\beta}_{32}$	-0.174 (0.099)	-0.112 (0.072)
			$\hat{\beta}_{33}$	-0.198 (0.090)	-0.146 (0.071)

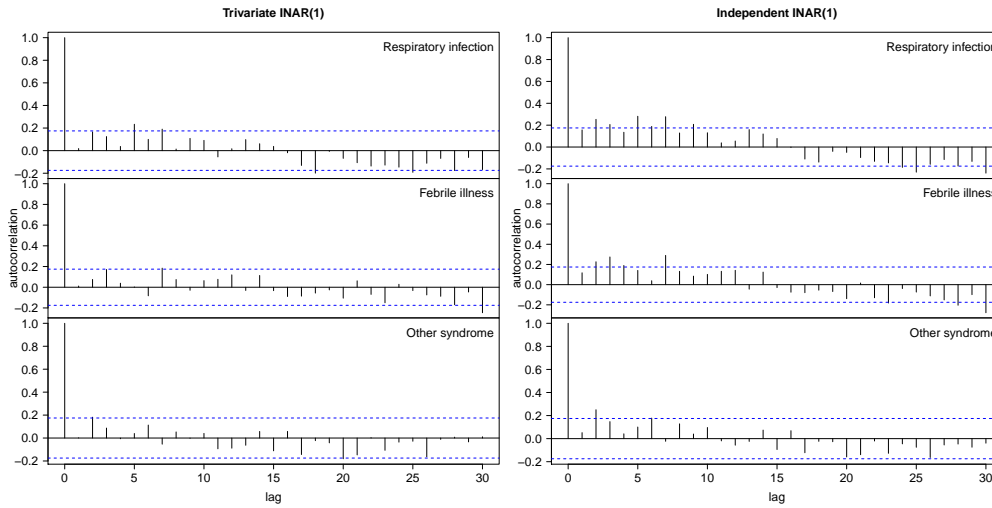


Figure 4: Plots of the autocorrelations of the residuals obtained by the trivariate INAR(1) (left panel) and the independent INAR(1) (right panel) regression models.



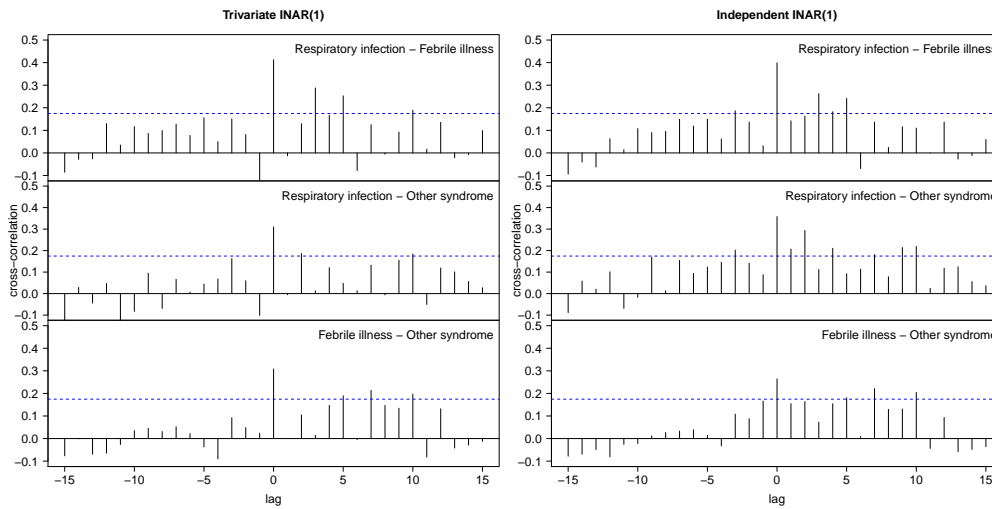


Figure 5: Plots of the cross-correlations of the residuals obtained by the trivariate INAR(1) (left panel) and the independent INAR(1) (right panel) regression models.

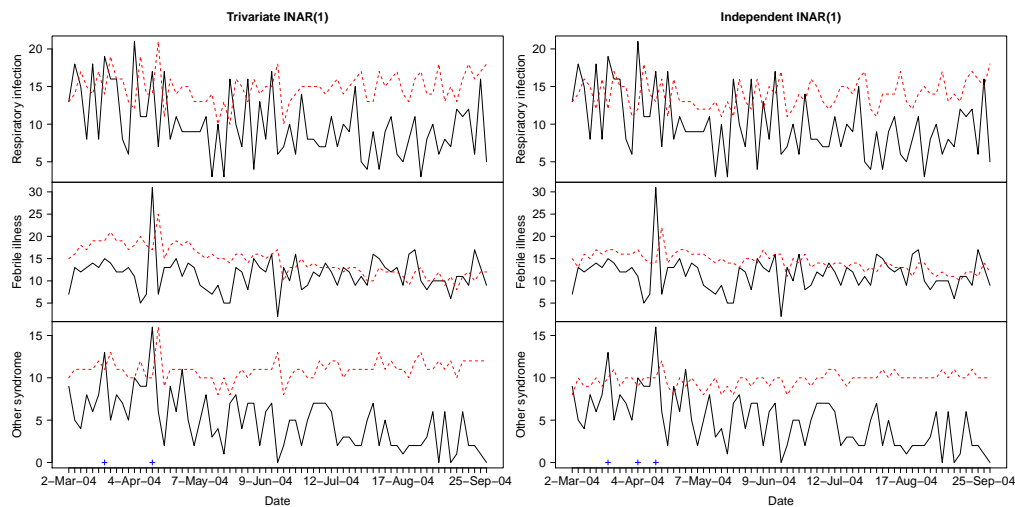


Figure 6: Surveillance plots as obtained after fitting a trivariate INAR(1) regression model with independent Poisson innovations (left panel) or three independent Poisson INAR(1) regression models (right panel) to the historical data. Statistical alarms (blue crosses) are raised when at least two series exceed the upper bounds of the corresponding 99% prediction intervals (red dashed lines).

## Acknowledgements

This project has received funding from the Athens University of Economics, Action II Funding & Research Funding Program no. 2938-01 and from the European Union's Horizon 2020 research and innovation programme under the Marie Skłodowska-Curie grant agreement no. 699980.

## References

- Al-Osh, M. and A. Alzaid (1987). First-Order Integer-Valued Autoregressive Process. *Journal of Time Series Analysis* 8, 261–275.
- Borrer, C., C. Champ, and S. Rigdon (1998). Poisson EWMA control charts. *Journal of Quality Technology* 30, 352–361.
- Cardinal, M., R. Roy, and J. Lambert (1999). On the application of integer-valued time series models for the analysis of disease incidence. *Statistics in Medicine* 18, 2025–2039.
- Choi, K. (1999). An evaluation of influenza mortality surveillance, 1962-1979: I: Time series forecasts of expected pneumonia and influenza deaths. *American Journal of Epidemiology* 113, 215–226.
- Cozzucoli, P. C. and M. Marozzi (2018). Monitoring multivariate poisson processes: a review and some new results. *Quality Technology & Quantitative Management* 15(1), 53–68.
- Dafni, U., S. Tsiodras, D. Panagiotakos, K. Gkolfinopoulou, G. Kouvatsas, Z. Tsourti, and G. Saroglou (2004). Algorithm for Statistical Detection of Peaks - Syndromic Surveillance System for the Athens 2004 Olympic Games. *MMWR. Morbidity and mortality weekly report* 53 (Suppl), 86–94.
- Das, D., D. Weiss, F. Mostashari, T. Treadwell, J. McQuiston, L. Hutwagner, A. Karpati, K. Bornschlegel, M. Seeman, R. Turcios, P. Terebuh, R. Curtis, R. Heffernan, and S. Balter (2003). Enhanced Drop-in Syndromic Surveillance in New York City Following September 11, 2001. *Journal of Urban Health: Bulletin of the New York Academy of Medicine* 80(Suppl 1), i76–i88.
- Farrington, C., N. Andrews, A. Beale, and M. Catchpole (1996). A statistical algorithm for the early detection of outbreaks of infectious disease. *Journal of the Royal Statistical Society: Series A* 159, 547–563.
- Franke, J. and T. S. Rao (1993). Multivariate first-order integer-valued autoregressions. *Technical report. Forschung Universitat Kaiserslautern*.
- Frisén, M. (2010). Principles for multivariate surveillance. In H. Lenz, P. Wilrich, and W. Schmid (Eds.), *Frontiers in Statistical Quality Control* 9, pp. 133–144. Berlin: Springer.

- Gesteland, P. H., R. M. Gardner, F.-C. Tsui, J. U. Espino, R. T. Rolfs, B. C. James, W. W. Chapman, A. W. Moore, and M. M. Wagner (2003). Automated Syndromic Surveillance for the 2002 Winter Olympics. *Journal of the American Medical Informatics Association* 10, 547–554.
- Gurland, J. (1957). Some interrelations among compound and generalized distributions. *Biometrika* 44, 265–268.
- Held, L., M. Hofmann, M. Höhle, and V. Schmid (2006). A two-component model for counts of infectious diseases. *Biostatistics* 7, 422–437.
- Held, L., M. Höhle, and M. Hofmann (2005). A statistical framework for the analysis of multivariate infectious disease surveillance counts. *Statistical Modelling* 5, 187–199.
- Held, L., S. Meyer, and J. Bracher (2017). Probabilistic forecasting in infectious disease epidemiology: the 13th armitage lecture. *Statistics in Medicine* 36(22), 3443–3460.
- Helfenstein, U. (1986). Box-Jenkins modelling of some viral infectious diseases. *Statistics in Medicine* 5, 37–47.
- Höhle, M. (2007). Surveillance: an R package for the monitoring of infectious diseases. *Computational Statistics* 22, 571–582.
- Höhle, M. and A. Mazick (2010). Aberration detection in R illustrated by Danish mortality monitoring. In T. Kass-Hout and X. Zhang (Eds.), *Biosurveillance: Methods and Case Studies*, pp. 215–237. London: CRC Press.
- Höhle, M. and M. Paul (2008). Count data regression charts for the monitoring of surveillance time series. *Computational Statistics and Data Analysis* 52, 4357–4368.
- Jackson, M., A. Baer, I. Painter, and J. Duchin (2007). A simulation study comparing aberration detection algorithms for syndromic surveillance. *BMC Medical Informatics and Decision Making* 7(6).
- Kemp, C. and A. Kemp (1965). Some properties of the ‘Hermite’ distribution. *Biometrika* 52, 381–394.
- Kokonendji, C. C. and P. Puig (2018). Fisher dispersion index for multivariate count distributions: A review and a new proposal. *Journal of Multivariate Analysis* 165, 180–193.
- Latour, A. (1997). The multivariate GINAR(p) process. *Advances in Applied Probability* 29, 228–248.
- Lucas, J. (1985). Counted data CUSUM’s. *Technometrics* 27, 129–144.
- McKenzie, E. (1985). Some Simple Models for Discrete Variate Time Series. *Water Resources Bulletin* 21, 645–650.

- Meyer, S., L. Held, and M. Höhle (2017). Spatio-Temporal Analysis of Epidemic Phenomena Using the R Package *surveillance*. *Journal of Statistical Software* 77(11), 1–55.
- Mundorff, M., P. Gesteland, M. Haddad, and R. Rolfs (2004). Syndromic Surveillance using Chief Complaints from Urgent-Care Facilities During the Salt Lake 2002 Olympic Winter Games. *MMWR. Morbidity and mortality weekly report* 53 (Suppl), 254.
- Noufaily, A., D. G. Enki, P. Farrington, P. Garthwaite, N. Andrews, and A. Charlett (2013). An improved algorithm for outbreak detection in multiple surveillance systems. *Statistics in Medicine* 32(7), 1206–1222.
- Parker, R. (1989). Analysis of surveillance data with Poisson regression: a case study. *Statistics in Medicine* 8, 285–294.
- Paul, M. and L. Held (2011). Predictive assessment of a non-linear random effects model for multivariate time series of infectious disease counts. *Statistics in Medicine* 30, 1118–1136.
- Paul, M., L. Held, and A. Toschke (2008). Multivariate modelling of infectious disease surveillance data. *Statistics in Medicine* 27, 6250–6267.
- Pedeli, X. and D. Karlis (2011). A bivariate INAR(1) process with application. *Statistical Modelling* 11, 325–349.
- Pedeli, X. and D. Karlis (2013a). On composite likelihood estimation of a multivariate INAR(1) model. *Journal of Time Series Analysis* 34, 206–220.
- Pedeli, X. and D. Karlis (2013b). Some properties of multivariate INAR(1) processes. *Computational Statistics and Data Analysis* 67, 213–225.
- Reis, B. and K. Mandl (2003). Time series modeling for syndromic surveillance. *BMC Medical Informatics and Decision Making* 3(2).
- Salmon, M., D. Schumacher, and M. Höhle (2016). Monitoring count time series in r: Aberration detection in public health surveillance. *Journal of Statistical Software* 70(10), 1–35.
- Schiöler, L. and M. Frisén (2012). Multivariate outbreak detection. *Journal of Applied Statistics* 39(2), 223–242.
- Shmueli, G. and H. Burkom (2010). Statistical challenges facing early outbreak detection in biosurveillance. *Technometrics* 52, 39–51.
- Siripanthana, S. (2013). *Sufficient reduction methods for multivariate health surveillance*. Ph. D. thesis, University of Sheffield.
- Sonesson, C. and D. Bock (2003). A review and discussion of prospective statistical surveillance in public health. *Journal of the Royal Statistical Society: Series A* 166, 5–21.

- Sonesson, C. and M. Frisé (2005). Multivariate surveillance. In A. B. Lawson and K. Kleinman (Eds.), *Spatial Surveillance for Public Health*, pp. 169–186. Chichester: Wiley.
- Strat, Y. L. and F. Carrat (1999). Monitoring epidemiologic surveillance data using hidden Markov models. *Statistics in Medicine* 18, 3463–3478.
- Unkel, S., C. Farrington, and P. Garthwaite (2012). Statistical methods for the prospective detection of infectious disease outbreaks: a review. *Journal of the Royal Statistical Society: Series A* 175, 49–82.
- Vial, F., W. Wei, and L. Held (2016). Methodological challenges to multivariate syndromic surveillance: a case study using Swiss animal health data. *BMC Veterinary Research* 12, 288.
- Wang, Z., Y. Li, and X. Zhou (2017). A statistical control chart for monitoring high-dimensional poisson data streams. *Quality and Reliability Engineering International* 33(2), 307–321.
- Watier, L., S. Richardson, and B. Hubert (1991). A time series construction of an alert threshold with application to *s. bovis* moribundus in France. *Statistics in Medicine* 10, 1493–1509.
- Weiß, C. (2009). EWMA monitoring of correlated process of Poisson counts. *Quality Technology & Qualitative Management* 6, 137–153.
- Weiß, C. (2011). Detecting mean increases in Poisson INAR(1) process with EWMA control charts. *Journal of Applied Statistics* 38, 383–398.
- Weiß, C. (2015). SPC methods for time-dependent processes of count—a literature review. *Cogent Mathematics* 2: 1111116.
- Weiß, C. and M. Testik (2009). CUSUM monitoring of first-order integer-valued autoregressive processes of Poisson counts. *Journal of Quality Technology* 41, 389–400.